Three-Dimensional Structure of the Ligand-Binding Core of GluR2 in Complex with the Agonist (*S*)-ATPA: Implications for Receptor Subunit Selectivity

Marie-Louise Lunn,[§,#] Anders Hogner,[§] Tine B. Stensbøl,[§] Eric Gouaux,[‡] Jan Egebjerg,[#] and Jette S. Kastrup[§,*]

Department of Medicinal Chemistry, Pharmaceutical University of Denmark, Universitetsparken 2, DK-2100 Copenhagen, Denmark, Department of Molecular and Structural Biology, C. F. Møllers Allé 130, University of Aarhus, DK-8000 Aarhus, Denmark, and Department of Biochemistry and Molecular Biophysics, Columbia University, 650 W. 168 Street, New York, New York 10032

Received August 6, 2002

Two X-ray structures of the GluR2 ligand-binding core in complex with (*S*)-2-amino-3-(5-*tert*-butyl-3-hydroxy-4-isoxazolyl)propionic acid ((*S*)-ATPA) have been determined with and without Zn^{2+} ions. (*S*)-ATPA induces a domain closure of ca. 21° compared to the apo form. The *tert*-butyl moiety of (*S*)-ATPA is buried in a partially hydrophobic pocket and forces the ligand into the glutamate-like binding mode. The structures provide new insight into the molecular basis of agonist selectivity between AMPA and kainate receptors.

Introduction

Glutamate receptors are abundant in the central nervous system and play a crucial role in normal brain function as well as for the mechanisms underlying various neurological and probably psychiatric disorders. The ionotropic glutamate receptors (iGluRs) are divided into 2-amino-3-(3-hydroxy-5-methyl-4-isoxazolyl)propionic acid (AMPA), kainate, and *N*-methyl-D-aspartic acid (NMDA) receptors, where the subunits GluR1−GluR4 form the AMPA receptors and the subunits GluR5−GluR7 and KA1−KA2 the kainate receptors.[1]

The iGluRs are tetrameric complexes comprised of dimers-of-dimers,[2] see Figure 1a. A soluble form of the ligand-binding core of GluR2 (GluR2-S1S2J), created by substitution of the transmembrane regions M1 and M2 by a peptide linker and exclusion of the amino-terminal domain and M3, shows pharmacological profiles comparable with that of the full-length membrane-bound receptor.[3−6] Subsequently, high-resolution X-ray structures of S1S2J in complex with different agonists and one antagonist have revealed different degrees of closure of the cleft between the two domains forming the ligand-binding core.[2,6,7]

The increasing understanding of the molecular diversity underlying the iGluR system has challenged the development of subtype selective ligands, and in this respect AMPA analogues have been studied extensively.[1] Systematic replacement of the isoxazole 5-substituent combined with electrophysiology experiments at recombinant receptors implies that the moiety at the 5-position drastically influences the selectivity between AMPA and kainate receptors.[8] AMPA only activates some kainate receptors and only at high concentrations, while the 5-*tert*-butyl derivative, (*S*)-2-amino-3-(5-*tert*-butyl-3-hydroxy-4-isoxazolyl)propionic acid ((*S*)-ATPA, Figure 1b), activates GluR5 receptors with more than 50-fold higher potency than the AMPA receptors.[9] To investigate the molecular mechanisms underlying the selectivity of (*S*)-ATPA between AMPA and kainate receptors, we have obtained two high-resolution X-ray structures of the GluR2-S1S2J in complex with this ligand in the presence and absence of Zn^{2+} ions, respectively.

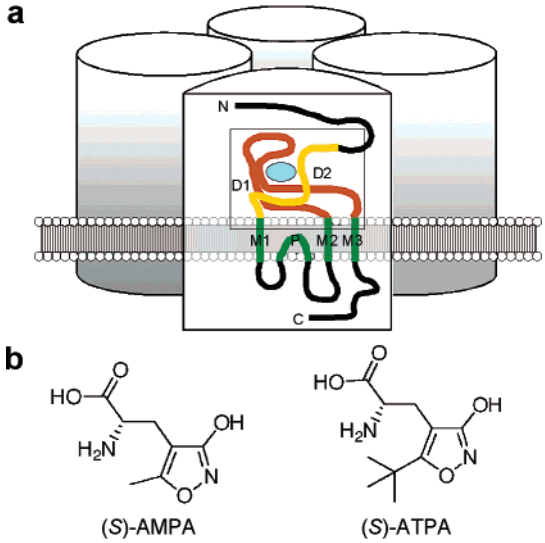

Figure 1. (a) Illustration of the tetrameric iGluR AMPA receptor topology. Each subunit has three transmembrane spanning regions (M1−M3, in green), a ligand-binding core comprised of segments S1 (in yellow) and S2 (in orange), and a re-entrant loop (P, in green) between M1 and M2. The ligand (blue oval) binds in a cleft formed by the two domains D1 and D2, composed of segments S1 and S2. (b) Chemical structures of (*S*)-AMPA and (*S*)-ATPA.

Results and Discussion

The correct folding of the GluR2-S1S2J protein was determined pharmacologically by saturation binding of [^{3}H]AMPA and by competitive displacement of the [^{3}H]-AMPA binding using (*S*)-ATPA. The binding affinity for AMPA (K_d is 10.9 ± 4.2 nM and B_{max} is 0.68 ± 0.06 pmol) and the IC_{50} value for (*S*)-ATPA were found to be in good agreement with AMPA receptor pharmacology[9,10] (Figure 2). The structure of GluR2-S1S2J in complex with the agonist (*S*)-ATPA was determined in the presence and absence of Zn^{2+} ions. The structures contain one (denoted MolA, zinc form) and two molecules (denoted MolB and MolC, zinc free form) in the asymmetric unit of the crystal. Pairwise superpositions of the Cα-atoms of the three molecules yield root-mean square deviations of 0.34−0.36 Å. The presence of two Zn^{2+} ions in the zinc form only to a minor extent

* To whom correspondence should be addressed: Tel: +45 35 30 64 86. Fax: +45 35 30 60 40. E-mail: jsk@dfh.dk.
§ Pharmaceutical University of Denmark.
# University of Aarhus.
‡ Columbia University.

10.1021/jm021020+ CCC: $25.00
Published on Web 01/30/2003

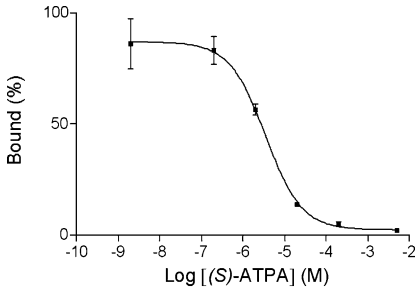

Figure 2. Competition binding characteristics of the GluR2-S1S2J protein: Diagram of the [^{3}H]AMPA displacement by (*S*)-ATPA. IC_{50} is 3.5 μM (1.9−6.3 μM).

Table 1. Crystal Data and Statistics for Data Collection and Refinements of the Two GluR2-S1S2J:(*S*)-ATPA Complexes

	zinc free form	zinc-containing form
Crystal Data		
space group	$P2_12_12$	$P2_12_12$
unit cell parameters (Å)	a = 96.7, b = 121.5, c = 47.1	a = 54.3, b = 111.2, c = 46.6
no. of molecules per au	2	1
Data Collection		
resolution range (Å)	20.0−1.90	20.0−1.85
number of unique reflns	40,611	23,016
average redundancy	4.1	3.5
completeness (%)[a]	92.2 (81.6)	92.6 (82.1)
R_{merge} (%)[a,b]	9.2 (34.8)	9.9 (34.0)
$I/\sigma(I)$[a]	13.1 (2.4)	7.0 (2.0)
Refinement		
total number of:		
non-hydrogen atoms	4,805	2,217
amino acid residues	516	258
ligand/Zn^{2+}/Cl^-/sulfate	2/0/0/2	1/2/1/0
water molecules	725	179
R-factor:		
R_{work}[c]	19.0 (86.4%)	20.7 (93.6%)
R_{free}[d]	21.7 (4.6%)	24.5 (2.7%)
rms deviations:		
bond lengths (Å)/angles (deg)	0.006/1.4	0.009/1.4
residues in allowed regions of Ramachandran plot (%)[e]	98.7	99.6
mean B-values (Å^2):		
protein atoms/ligand atoms	19.4/16.7	26.8/22.6

[a] Numbers in parentheses are for the outermost bin; zinc free crystal form: 1.97−1.90 Å and zinc-containing form: 1.92−1.85 Å. [b] $R_{merge}(I) = \sum_{hkl}|I_{hkl} - \langle I_{hkl}\rangle|/\sum_{hkl}I_{hkl}$ [c] $R = \sum_{hkl}||F_o| - |F_c||/\sum|F_o|$, where $|F_o|$ and $|F_c|$ are observed and calculated structure factor amplitudes, respectively, for reflection *hkl*. [d] 5 and 3% of the reflections in the zinc free and zinc-containing structures, respectively, were set aside for calculation of the R_{free} value. [e] The Ramachandran plots were calculated according to Kleywegt and Jones.[25]

influences the structure of GluR2-S1S2J in agreement with results recently reported of an agonist complex.[11]

Interactions between (*S*)-ATPA and the GluR2−S1S2J Ligand-Binding Site. The same binding mode of (*S*)-ATPA is revealed in the two GluR2-S1S2J X-ray structures presented. (*S*)-ATPA interacts with the ligand-binding site of GluR2 by an extensive number of direct contacts. The interactions are very similar in all three molecules (Table 2: MolA-C, Figure 3). The α-carboxylate group of the glutamate backbone interacts through a total of four potential hydrogen bonds/ion pairs to Thr480, Arg485, and Ser645. A tetrahedral arrangement is established to the α-ammonium group of the ligands via hydrogen bonds to Pro478, Thr480, and Glu705. The interactions between the α-carboxylate and α-ammonium groups of the ligand and the binding site are similar to those of the previously described agonist complexes.[6,7]

Table 2. Interactions of (*S*)-ATPA with the Ligand-Binding Core of GluR2-S1S2J. Potential Hydrogen Bonds/Ionic Interactions to Ligand within 3.3 Å Are Tabulated

	zinc-containing form	zinc free form	
	MolA	MolB	MolC
carboxylate oxygen **1**[a]			
Arg485 Nη1	2.8	2.7	2.7
Thr480 N	2.9	2.8	3.1
carboxylate oxygen **2**[a]			
Arg485 Nη2	2.8	2.8	2.9
Ser654 N	2.7	2.9	2.7
ammonium group[b]			
Pro478	2.9	2.8	2.9
Thr480 Oγ	2.8	2.8	2.7
Glu705 Oϵ1	3.1	3.3	3.4
Glu705 Oϵ2	2.6	2.8	2.9
hydroxy oxygen[c]			
Thr655 N	3.1	3.2	3.2
Thr655 Oγ	3.1	3.0	2.9
water 1	2.9	2.9	2.9
ring nitrogen[c]			
Thr655 Oγ	3.1	2.9	3.0
water 2	2.9	2.8	2.8

[a] Atoms of the α-carboxylate group of ligand. [b] Atoms of the α-ammonium group of ligand. [c] Heteroatoms of the isoxazolol ring of ligand.

In the GluR2-S1S2J structures, the hydroxyl group at the isoxazole ring occupies a position similar to that occupied by one of the oxygen atoms of the γ-carboxylate moiety in the (*S*)-glutamate complex.[6] The hydroxyl group binds to D2 via two direct hydrogen bonds to Thr655, as well as indirectly through a water molecule (W1, Table 2 and Figure 3a). The water molecule W1 makes further hydrogen bonds to the oxygen atom of Leu650 and to the backbone nitrogen of Lys656. The isoxazole moiety in (*S*)-ATPA is situated considerably closer to D2 (distance between hydroxyl group and Thr655 Cα is ca. 3.8 Å) compared to the isoxazole moiety in (*S*)-AMPA (ca. 4.5 Å) and the interactions of (*S*)-ATPA thereby resembles the (*S*)-glutamate mode of interaction and not the (*S*)-AMPA mode (Figure 3).[6] The interaction with D2 is further stabilized by two hydrogen bonds between the isoxazole ring-nitrogen atom and Thr655 and a water molecule (W2), enabling indirect contact to Thr649, Leu650, Tyr702, and Leu703.

The *tert*-butyl moiety in the 5-position of (*S*)-ATPA points toward a partly hydrophobic pocket[7] and makes van der Waals interactions with Glu402 (closest contact to Oϵ1), Tyr450 (Oη), and Pro478 (Cγ) in D1 and to Leu650 (Cδ2), Thr686 (Oγ1), Glu705 (Oϵ2), Met708 (Cβ), and Tyr732 (Oη) in D2 (Table 3). It is evident from the shape of the partially hydrophobic cavity encompassing the *tert*-butyl moiety that bulky substituents at the 5-position cannot be accommodated if the ligand binds in the (*S*)-AMPA mode. As a result, the isoxazolol hydroxy group displaces the water molecule that forms the tight association between the isoxazolol hydroxy group in (*S*)-AMPA and the protein.[6] In addition, ligands might also interfere with Leu650 and the Glu402-Thr686 interdomain interaction to various degrees depending on the size and bulkiness of the substituent. As for the agonist complex structures solved to date,[6,7] this interdomain lock is maintained in the two (*S*)-ATPA structures.

Implications for Receptor Subunit Selectivity. (*S*)-ATPA is the most commonly used selective GluR5 agonist, with a 20−50-fold higher potency for GluR5 than for the AMPA receptors,[9] implying that the bulky *tert*-butyl group is well accommodated by the ligand-binding site of GluR5. Eight amino acid residues are involved in van der Waals interactions to the *tert*-butyl

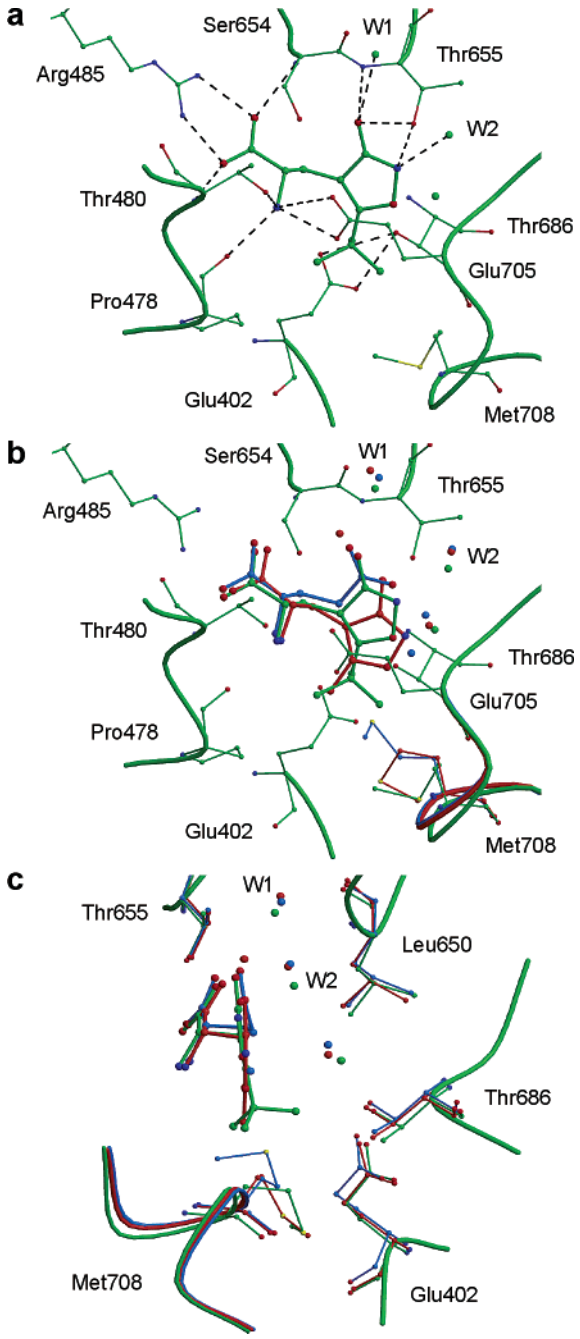

Figure 3. The ligand-binding site of GluR2-S1S2J. (a) The (*S*)-ATPA complex, using MolB as a representative. Heteroatoms are in standard colors (nitrogen is blue, oxygen is red, and sulfur is green). Water molecules are displayed as green spheres, and dashed lines indicate potential hydrogen bonds/ionic interactions listed in Table 2. (b) Superimposition of the (*S*)-ATPA (in green), (*S*)-glutamate (in blue), and (*S*)-AMPA (in orange) complexes. (c) As in b, but rotated ca. 90° about a vertical axis.

group (Table 3) of which Leu650, Thr686, and Met708 are replaced by the smaller amino acids Val(685), Ser(721), and Ser(741), respectively, in GluR5. Results from mutagenesis studies performed on GluR1 show that Ser741 in GluR5 is the main determinant for the selective profile of ATPA.[12] In accordance, we observe that the side chain of Met708 is reoriented further away from (*S*)-ATPA compared to the (*S*)-glutamate or (*S*)-AMPA structures (Figure 3b,c). Modeling studies suggest that the hydroxyl group of a serine at position 708 might, even in the presence of the *tert*-butyl group, form

Table 3. Residues of the Ligand-Binding Core of GluR2-S1S2J in van der Waals Contacts (4 Å) of (*S*)-ATPA. Comparison of Equivalent Residues among All Known AMPA (GluR1−4) and Kainate (GluR5−7 and KA1−2) Receptors

GluR2	GluR1/GluR3/GluR4	GluR5/GluR6/GluR7	KA1/KA2
Glu402[c]	Glu	Glu	Glu
Tyr450[a,c]	Tyr	Tyr	Tyr
Pro478[a,c−d]	Pro	Pro	Gly/Ala
Leu479[a]	Leu	Leu	Leu/Phe
Thr480[a,d]	Thr	Thr/Ala/Thr	Thr
Arg485[a,d]	Arg	Arg	Arg
Thr649[e−f]	Thr	**Ala**	Thr
Leu650[b,c,e,g]	Leu	**Val**	Ile
Gly653[a,b]	Gly	Gly	Gly
Ser654[a,b,d]	Ser	Ser/Ala/Ala	Ser
Thr655[b,d,g]	Thr	Thr	Ser/Thr
Lys656[e−f]	Lys	**Met**	Met
Thr686[c,e]	Thr	**Ser**/Asn/Asn	Thr
Tyr702[e−f]	Tyr/Phe/Phe	**Leu**/Phe/Leu	Phe
Leu703[f]	Leu	Leu	Leu
Leu704[b,e]	Leu	**Met**	Leu
Glu705[a−d]	Glu	Glu	Glu
Met708[c,e]	Met	**Ser**/Thr/Thr	Met
Tyr732[a,c]	Tyr	Tyr	Tyr

[a] The residue makes contact to the amino acid part of ligand. [b] The residue makes contact to the isoxazolol ring of ligand. [c] The residue makes contact to the *tert*-butyl group of ligand. [d] The residue makes a direct hydrogen bond to ligand. [e] Residues listed in bold differ between the GluR2 and GluR5 subunits. [f] The residue makes a water-mediated hydrogen bond to ligand, but is further away than 4.0 Å. [g] The residue makes a water-mediated hydrogen bond to ligand.

an indirect hydrogen bond to Tyr405 through a water molecule and thereby stabilizes the domain closure by formation of an additional interdomain interaction between D1 and D2. Additional selectivity also might be imposed by the interaction between Leu650 and the ring-oxygen atom in the isoxazole ring.

Domain Closure and Dimerization of GluR2-S1S2J. The agonist (*S*)-ATPA introduces ca. 21° domain closure (MolA: 21.4°, MolB: 21.7°, and MolC: 21.2°) relative to the apo structure of GluR2-S1S2J (PDB id-code: 1FTO, molecule A). It has been shown that the domains of the ligand-binding core close upon agonist binding,[2,6,7] and the degree of closure observed for (*S*)-ATPA is similar to that of (*S*)-glutamate and (*S*)-AMPA. As in the structure of (*S*)-AMPA, the trans peptide bond between Asp651 and Ser652 has flipped approximately 180° compared to the apo structure of GluR2-S1S2J. In both (*S*)-ATPA structures, 2-fold dimers with interface accessible surface areas of 875 and 889 Å^2 per monomer for the zinc free and zinc-containing structures, respectively, are formed and the dimer interfaces are similar to those previously reported.[2,6,7]

Conclusion

High-resolution X-ray structures have been determined of the GluR2 ligand-binding core S1S2J in complex with the isoxazolol-containing agonist (*S*)-ATPA in the presence and absence of Zn^{2+} ions. The detailed information on the interactions of (*S*)-ATPA with the receptor has increased our understanding of the selectivity between AMPA and kainate receptors and furthermore will facilitate the design of new, subunit-selective ligands.

Experimental Section

Materials. (*S*)-ATPA was synthesized and resolved as described[9] and kindly provided by colleagues from the Department of Medicinal Chemistry. AMPA was a gift from P. Krogsgaard-Larsen, and the general chemicals were purchased from Sigma.

Expression and Purification. The GluR2-S1S2J construct developed by Armstrong et al.[6] was used, and the protein was expressed, refolded, and purified essentially as reported.[4,13]

[^{3}H]AMPA Binding. Ligand binding was performed as previously described.[4] For saturation binding, triplets of refolded GluR2-S1S2J protein (0.08 mg/mL) was incubated for 1 h on ice with 1−200 nM [^{3}H]AMPA (11.1 Ci/mmol, NEN Boston) in binding buffer (100 mM thiocyanate, 2.5 mM $CaCl_2$, and 30 mM Tris-HCl pH 7.2) to a total volume of 500 μL. Competition experiments were employed under similar conditions, using 20 nM [^{3}H]AMPA and 2 nM−5 mM (*S*)-ATPA. Nonspecific binding was measured in the presence of 1 mM glutamate.

Crystallization. GluR2-S1S2J in complex with (*S*)-ATPA was crystallized by the hanging drop vapor diffusion method at 6 °C. The protein complex solution contained 8 mg/mL GluR2-S1S2J and 1.4 mg/mL (*S*)-ATPA (molar ratio 1:25) in 10 mM Hepes pH 7.4, 20 mM sodium chloride, and 1 mM EDTA. Crystals were obtained in drops consisting of 1 μL complex solution and 1 μL reservoir solution of 0.1 M zinc acetate, 0.1 M cacodylate buffer pH 5.5, and 20% PEG 8000. The reservoir volume was 0.5 mL. The crystals grew within one week to a maximum dimension of 0.1 mm. In general, crystals without Zn^{2+} ions were obtained as described above, but by using a reservoir solution of 0.1 M ammonium sulfate, 0.1 M sodium acetate pH 5.6, and 18% PEG 8000.

Data Collection. The data of GluR2-S1S2J in complex with (*S*)-ATPA were collected on beamline I711 at MAX Lab, Lund, at 100 K using a MAR345 image plate detector and wavelength of 1.0760 Å for the zinc free crystal form and 1.0232 Å for the zinc-containing crystal form, respectively. The crystals were transferred to a cryo-solution containing 15% glycerol, the ligand, and reservoir solution for a few seconds prior to flash-cooling. A full data set of the zinc free form was collected to 1.90 Å resolution and of the zinc form to 1.85 Å as two different data sets: A low- and a high-resolution set. The low-resolution data set was collected in resolution range 20.0−3.2 Å, whereas the high-resolution data set was covering data from 20.0 to 1.85 Å. All data were autoindexed and processed with the HKL programs DENZO and SCALEPACK.[14] For crystal data and data collection statistics, see Table 1.

Structure Determination and Refinements. Both structures were solved by molecular replacement, using the program AMoRe[15] from CCP4.[16] The structure of GluR2-S1S2J in complex with the ligand (*S*)-thio-ATPA (Lunn et al., to be published) was used as search model for phasing the data of the zinc-containing form, including protein atoms only. The structure of the zinc free form was solved using the structure of the zinc form as search model (protein atoms only), resulting in two clear solutions. Initially, the amino acid residues were traced using ARP/wARP[17] except for a few amino acids, which were manually built using program O.[18] In addition, the ligand was unambiguously fitted into the electron densities. The structure was further subjected to refinements in CNS,[19] each step comprising positional and B-factor refinements. Between each refinement step, the structures were inspected and corrected using program O. Gradually, water molecules, as well as Zn^{2+}, Cl^-, and sulfate ions, were added to the structures. The structures comprise amino acid residues 393−506 from segment S1 of the membrane-bound receptor, a two amino acid linker Gly-Thr, and residues 632−773 from segment S2. A summary of the structure refinements is presented in Table 1. Coordinates have been deposited in the Protein Data Bank (ID codes 1NNK and 1NNP).

The HINGEFIND script[20] implemented in the program-VMD[21] was employed for analysis of ligand-induced domain closure. The interface-accessible surface areas were generated by the Protein Interaction Server.[22] Figures were prepared with Molscript[23] and Raster3d.[24]

Acknowledgment. We thank Dr. Jeremy R. Greenwood for guidance using computational techniques for generating ligand parameters. The work was supported by grants from NeuroScience PharmaBiotec, The Dansync Center for Synchrotron Radiation, Apotekerfonden of 1991, The Danish Medical Research Council, Novo Nordisk Fonden, and The European Community − Access to Research Infrastructure Action of the Improving Human Potential Programme.

References

(1) Bräuner-Osborne, H.; Egebjerg, J.; Nielsen, E. Ø.; Madsen, U.; Krogsgaard-Larsen, P. Ligands for glutamate receptors: Design and therapeutic prospects. *J. Med. Chem.* **2000**, *43*, 2609−2645.
(2) Sun, Y.; Olson, R.; Horning, M.; Armstrong, N.; Mayer, M.; Gouaux, E. Mechanism of glutamate receptor desensitization. *Nature* **2002**, *417*, 245−253.
(3) Kuusinen, A.; Arvola, M.; Keinänen, K. Molecular dissection of the agonist binding site of an AMPA receptor. *EMBO J.* **1995**, *14*, 6327−6332.
(4) Chen, G. Q.; Gouaux, E. Overexpression of a glutamate receptor (GluR2) ligand binding domain in *Escherichia coli*: Application of a novel protein folding screen. *Proc. Natl. Acad. Sci. U.S.A.* **1997**, *94*, 13431−13436.
(5) Amstrong, N.; Sun, Y.; Chen, G. Q.; Gouaux, E. Structure of a glutamate-receptor ligand-binding core in complex with kainate. *Nature* **1998**, *395*, 913−917.
(6) Armstrong, N.; Gouaux, E. Mechanisms for activation and antagonism of an AMPA-sensitive glutamate receptor: Crystal structures of the GluR2 ligand binding core. *Neuron* **2000**, *28*, 165−181.
(7) Hogner, A.; Kastrup, J. S.; Jin, R.; Liljefors, T.; Mayer,M. L.; Egebjerg, J.; Larsen, I. K.; Gouaux, E. Structural basis for AMPA receptor activation and ligand selectivity: Crystal structures of five agonist complexes with the GluR2 ligand binding core. *J. Mol. Biol.* **2002**, *322*, 93−109.
(8) Madsen, U.; Stensbøl, T. B.; Krogsgaard-Larsen, P. Inhibitors of AMPA and kainate receptors. *Curr. Med. Chem.* **2001**, *8*, 1291−1301.
(9) Stensbøl, T. B.; Johansen, T. N.; Egebjerg, J.; Ebert, B.; Madsen, U.; Krogsgaard-Larsen, P. Resolution, absolute stereochemistry and molecular pharmacology of the enantiomers of ATPA. *Eur. J. Pharmacol.* **1999**, *380*, 153−162.
(10) Keinänen, K.; Wisden, W.; Sommer, B.; Werner, P.; Herb, A.; Verdoorn, T. A.; Sakmann, B.; Seeburg, P. H. A family of AMPA-selective glutamate receptors. *Science* **1990**, *249*, 556−560.
(11) Kasper, C.; Lunn, M.-L.; Liljefors, T.; Gouaux, E.; Egebjerg, J.; Kastrup, J. S. GluR2 ligand-binding core complexes: Importance of the isoxazolol moiety and 5-substituent for the binding mode of AMPA-type agonists. *FEBS Lett.* **2002**, *531*, 173−178.
(12) Nielsen, M. M.; Liljefors, T.; Krogsgaard-Larsen, P.; Egebjerg, J. The selective activation of the glutamate receptor GluR5 by ATPA is controlled by serine 741. *Mol. Pharmacol.* **2002**, in press.
(13) Chen, G. Q.; Sun, Y.; Jin, R.; Gouaux, E. Probing the ligand binding domain of the GluR2 receptor by proteolysis and deletion mutagenesis defines domain boundaries and yields a crystallizable construct. *Protein Sci.* **1998**, *7*, 2623−2630.
(14) Otwinowski, Z.; Minor, W. Processing of X-ray diffraction data collected in oscillation mode. *Methods Enzymol.* **1997**, *276*, 307−326.
(15) Navaza, J. AMoRe: An automated package for molecular replacement. *Acta Crystallogr.* **1994**, *A50*, 157−163.
(16) Collaborative Computational Project, Number 4. The CCP4 Suite: Programs for Protein Crystallography. *Acta Crystallogr.* **1994**, *D50*, 760−763.
(17) Perrakis, A.; Morris, R.; Lamzin, V. S. Automated protein model building combined with iterative structure refinement. *Nat. Struct. Biol.* **1999**, *6*, 458−463.
(18) Jones, T. A.; Zou, J. Y.; Cowan, S. W.; Kjeldgaard, M. Improved methods for binding protein models in electron density maps and the location of errors in these models. *Acta Crystallogr.* **1991**, *A47*, 110−119.
(19) Brünger, A. T.; Adams, P. D.; Clore, G. M.; DeLano, W. L.; Gros, P.; Grosse-Kunstleve, R. W.; Jiang, J. S.; Kuszewski, J.; Nilges, M.; Pannu, N. S.; Read, R. J.; Rice, L. M.; Simonson, T.; Warren, G. L. Crystallography & NMR system: A new software suite for macromolecular structure determination. *Acta Crystallogr.* **1998**, *D54*, 905−921.
(20) Wriggers, W.; Schulten, K. Protein domain movements: Detection of rigid domains and visualization of hinges in comparisons of atomic coordinates. *Proteins* **1997**, *29*, 1−14.
(21) Humphrey, W.; Dalke, A.; Schulten, K. VMD−Visual molecular dynamics. *J. Mol. Graphics* **1997**, *14*, 33−38. http://www.ks.uiuc.edu/Research/vmd.
(22) Jones, S.; Thornton, J. M. Principles of protein−protein interactions. *Proc. Natl. Acad. Sci. U.S.A.* **1996**, *93*, 13−20. http://www.biochem.ucl.ac.uk/bsm/PP/server/.
(23) Kraulis, P. J. Molscript: A program to produce both detailed and schematic plots of protein structures. *J. Appl. Crystallogr.* **1991**, *24*, 946−950.
(24) Merritt, E. A.; Murphy, M. E. P. Raster3D version 2.0. A program for photorealistic molecular graphics. *Acta Crystallogr.* **1994**, *D50*, 869−873.
(25) Kleywegt, G. J.; Jones, T. A. Phi/Psi-chology: Ramachandran revisited. *Structure* **1996**, *4*, 1395−1400.

JM021020+